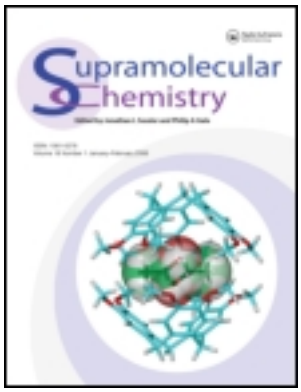

Supramolecular Chemistry
Publication details, including instructions for authors and subscription information:
http://www.tandfonline.com/loi/gsch20

Solid-state hydrogen-bonding self-assemblies and keto-enol tautomerism of 1,3-dipyrrolyl-1,3-propanediones

Yohei Haketa [a], Nazuki Eifuku [a], Yuya Bando [a], Ippei Yamada [a], Ayano Hagihara [a] & Hiromitsu Maeda [a b]

[a] College of Pharmaceutical Sciences, Institute of Science and Engineering, Ritsumeikan University, Kusatsu, 525-8577, Japan

[b] PRESTO, Japan Science and Technology Agency (JST), Kawaguchi, 332-0012, Japan

Published online: 13 Apr 2011.

To cite this article: Yohei Haketa, Nazuki Eifuku, Yuya Bando, Ippei Yamada, Ayano Hagihara & Hiromitsu Maeda (2011) Solid-state hydrogen-bonding self-assemblies and keto-enol tautomerism of 1,3-dipyrrolyl-1,3-propanediones, Supramolecular Chemistry, 23:03-04, 209-217, DOI: 10.1080/10610278.2010.521834

To link to this article: http://dx.doi.org/10.1080/10610278.2010.521834

Supramolecular Chemistry
Vol. 23, Nos. 3–4, March–April 2011, 209–217

Solid-state hydrogen-bonding self-assemblies and keto–enol tautomerism of 1,3-dipyrrolyl-1,3-propanediones

Yohei Haketa[a], Nazuki Eifuku[a], Yuya Bando[a], Ippei Yamada[a], Ayano Hagihara[a] and Hiromitsu Maeda[ab]*

[a]*College of Pharmaceutical Sciences, Institute of Science and Engineering, Ritsumeikan University, Kusatsu 525-8577, Japan;*
[b]*PRESTO, Japan Science and Technology Agency (JST), Kawaguchi 332-0012, Japan*

(*Received 6 July 2010; final version received 25 August 2010*)

Single-crystal X-ray analyses of various 1,3-dipyrrolyl-1,3-propanedione derivatives confirmed the formation of keto-based 1D N—H···O═C hydrogen-bonding chains and *cis*-enol-based hydrogen-bonding chains. The preferences for keto and enol tautomers in the solid state were found to depend significantly on the positions of substituents at pyrrole rings. α-Aryl-substituted derivatives afford keto forms, while β-alkyl- and β-aryl-substituted derivatives provide *cis*-enol forms.

Keywords: hydrogen bonding; pyrrole; self-assembly; supramolecular chemistry; tautomerism

1. Introduction

Hydrogen bonding is an essential non-covalent interaction that allows for the fabrication of biomacromolecular systems such as DNA double helices and protein folding structures and artificial supramolecular assemblies, including both crystals and soft materials (*1, 2*). In biotic and artificial systems, appropriately designing and arranging the hydrogen-bonding donor and acceptor sites in building components are crucial. One way to control hydrogen-bonding sites is through controlling tautomerism, the equilibrium between two or more states by intramolecular proton transfer. The equilibrium between a keto form and an enol form is a classic example of tautomerism and has been well studied (*3*). In particular, keto–enol tautomerism in linear 1,3-propanediones exhibits transition between mainly flexible keto forms and fairly rigid *cis*-enol forms with intramolecular hydrogen bonding. In the keto form, carbonyl oxygen moieties can behave as hydrogen-bonding acceptors, whereas, in the *cis*-enol form, hydroxy oxygen moieties contribute to the hydrogen-bonding interaction, but to a lesser extent.

The component of supramolecular assemblies, pyrrole, which is a π-conjugated heterocycle composed of functional biotic dyes such as haem and chlorophyll (*4*), affords various types of cyclic and acyclic anion receptors consisting of pyrrole ring(s) on the basis of the hydrogen-bonding donor NH site (*5*). Furthermore, self-assembled supramolecular networks of acyclic pyrrole derivatives with carbonyl groups at α-positions have been observed in the solid state as well as in the solution state (*6*). Therefore, increasing hydrogen-bonding sites, e.g. by the addition of pyrrole to 1,3-propanediones, would afford various supramolecular assemblies. For example, 1,3-dipyrrolyl-1,3-propanediones (dipyrrolyldiketones; e.g. **1a**; Figure 1(a)) (*7*), which are the essential precursors of anion-responsive boron complexes (*8, 9*) and pyrazole derivatives (*10*) (Figure 1(b)), form 1D N—H···O═C hydrogen-bonding chains and organised structures in the solid state (*11*). In this case, pyrrole NH acts as a hydrogen-bonding donor that is coplanar and faces the same side as the proximal carbonyl unit. A previous study reported that various pyrrole rings can be introduced in the core 1,3-propanedione spacer (*11*). Similar to other 1,3-propanedione derivatives, keto–enol equilibria were observed in the solution state for these dipyrrolyldiketones. Control of keto–enol equilibria in solution and in the solid state enables the tuning of electronic and optical properties for fabrication of functional materials. However, enol tautomers of dipyrrolyldiketones have not been observed in the solid state thus far, presumably due to the formation of more stable intermolecular hydrogen bonding using keto carbonyl moieties. These initial findings have been used as a basis for the control of solid-state assembled structures and keto–enol tautomerism in an attempt to modify pyrrole rings.

2. Results and discussion

2.1 Solid-state hydrogen-bonding assemblies of α-aryl derivatives

As reported in a previous study, alkyl substitution at pyrrole α-positions as seen in **1b** (Figure 2) provides sheet-like solid-state organised structures for aliphatic chains ($n = 10, 12, 14, 16$) (*11*). In addition to alkyl chains, aryl moieties can extend π-planes and, essentially, behave as platforms to connect various substituents to the dipyrrolyldiketone core. We obtained single crystals of phenyl **2a**, 2,6-dimethylphenyl **2b**

*Corresponding author. Email: maedahir@ph.ritsumei.ac.jp

ISSN 1061-0278 print/ISSN 1029-0478 online

DOI: 10.1080/10610278.2010.521834
http://www.informaworld.com

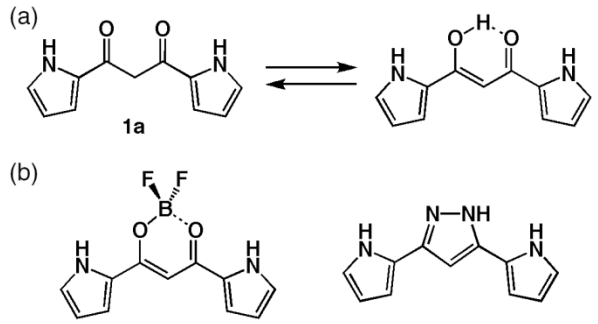

Figure 1. (a) Keto-enol tautomerism of dipyrrolyldiketone **1a** as the parent structure and (b) dipyrrolyldiketone-based BF_2 complex and pyrazole derivative.

(*9e*), *o*,*m*,*p*-methoxyphenyl **3a**–**c** and *m*,*p*-octyloxyphenyl **3d**,**e** (*9m*). These diketones were synthesised from the corresponding pyrrole derivatives and malonyl chloride in CH_2Cl_2. As with the single-crystal structure of **1a** (*9a, 11*), those of α-aryl derivatives **2a**,**b** and **3a**–**e** exhibit keto forms in the solid state (Figure 3). The intramolecular dihedral angles between two planes consisting of five atoms (NH and CO with the bridging pyrrole α-C) were estimated to be 64.18°, 99.98°, 50.68°, 85.60°, 74.07°, 58.36° and 53.32° for **2a**,**b** and **3a**–**e**, respectively; these values are smaller than those of **1a** at 109.01° and 102.67°. Between two pyrrole rings, **2a**,**b** and **3a**–**e** had almost the same values to each angle of the above planes at 61.92°, 100.32°, 49.83°, 84.37°, 79.22°, 54.03° and 53.21°, respectively. Furthermore, the peripheral aryl rings of **2a** are almost planar to the connecting pyrrole ring at 3.07° and 5.51°. In contrast, the 2,6-dimethylphenyl rings of **2b** show significant distortion from the pyrrole planes at 84.44° and 76.16°; this is possible due to the steric hindrance between *o*-CH_3 and the pyrrole NH or pyrrole β-CH unit. The corresponding values for **3a**–**e** are 22.49° for **3a**, 17.19° for **3b**, 2.57° and 7.44° for **3c**, 2.02° and 8.93° for **3d** and 25.45° for **3e**. *o*-Methoxy moieties of **3a** facing the pyrrole NH site exhibit intramolecular hydrogen-bonding N—H···O interactions.

The diketones **2a**,**b** and **3a**–**e** form 1D intermolecular hydrogen-bonding assemblies using pyrrole NH and diketone CO moieties (Figure 4). The distances between N(H) and (C)O are 2.92 and 2.95 Å for **2a**, 2.84 and 2.85 Å for **2b**, 2.94 Å for **3a**, 3.00 Å for **3b**, 2.87 and 2.93 Å for **3c**, 2.91 and 3.04 Å for **3d** and 2.95 Å for **3e**. Some of the diketones show weak intermolecular hydrogen bonding between aryl *o*-CH and carbonyl oxygen with the C(—H)···O distances of 3.35 and 3.36 Å for **2a**, 3.21 Å for **3b**, 3.41 and 3.42 Å for **3c**, 3.25 and 3.31 Å for **3d** and 3.43 Å for **3e**. The values of distances, as well as angles, of hydrogen-bonding assemblies are essential for exhibiting the versatility of the assembled structures depending on the pyrrole substituents. Regularly assembled structures are repeated by each *two* molecules in **1a**; the diketone **1a**, with chirality due to the twisted methylene (CH_2) unit, interacts with neighbouring enantiomers to afford racemic strands consisting of the *RSRS*··· configuration. Similar to **1a**, α-aryl-substituted **2a**,**b** and **3b**–**e** also form racemic wires of the *RSRS*··· configuration. In contrast, **3a** exhibits the formation of the equimolar chiral columns *RRRR*··· and *SSSS*···, wherein *o*-methoxy moieties are located at the *valley* zone constructed by π-conjugated moieties. Hydrogen-bonding planes of **3a** comprising NH and CO with the bridging pyrrole α-C are intermolecularly distorted at 50.68°, which is in sharp contrast to the completely parallel arrangements in **2a** and **3b**–**e**, where the parallel distances of the corresponding planes are 0.81, 0.74, 0.20, 0.29 and 0.028 Å, respectively. In addition, the planes are almost parallel in **2b** with the dihedral angle of 3.60°. Due to the distortion around the sp^3-CH_2 unit between two pyrrole moieties, hydrogen-bonding chains for **2a**,**b** and **3b**–**e** show alternating crinkled structures. For *m*-octyloxyphenyl **3d**, alkyl chains of each hydrogen-bonding chain are almost completely interdigitated to form lamella-like structures; in contrast, *p*-octyloxyphenyl **3e** exhibits layer structures assisted by partial interactions between alkyl chains.

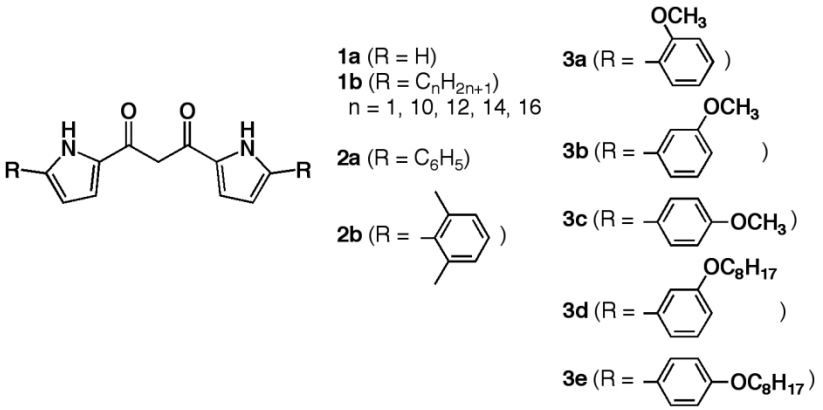

Figure 2. α-Aryl-substituted dipyrrolyldiketones **2a**,**b** and **3a**–**e** along with parent **1a** and α-alkyl **1b**.

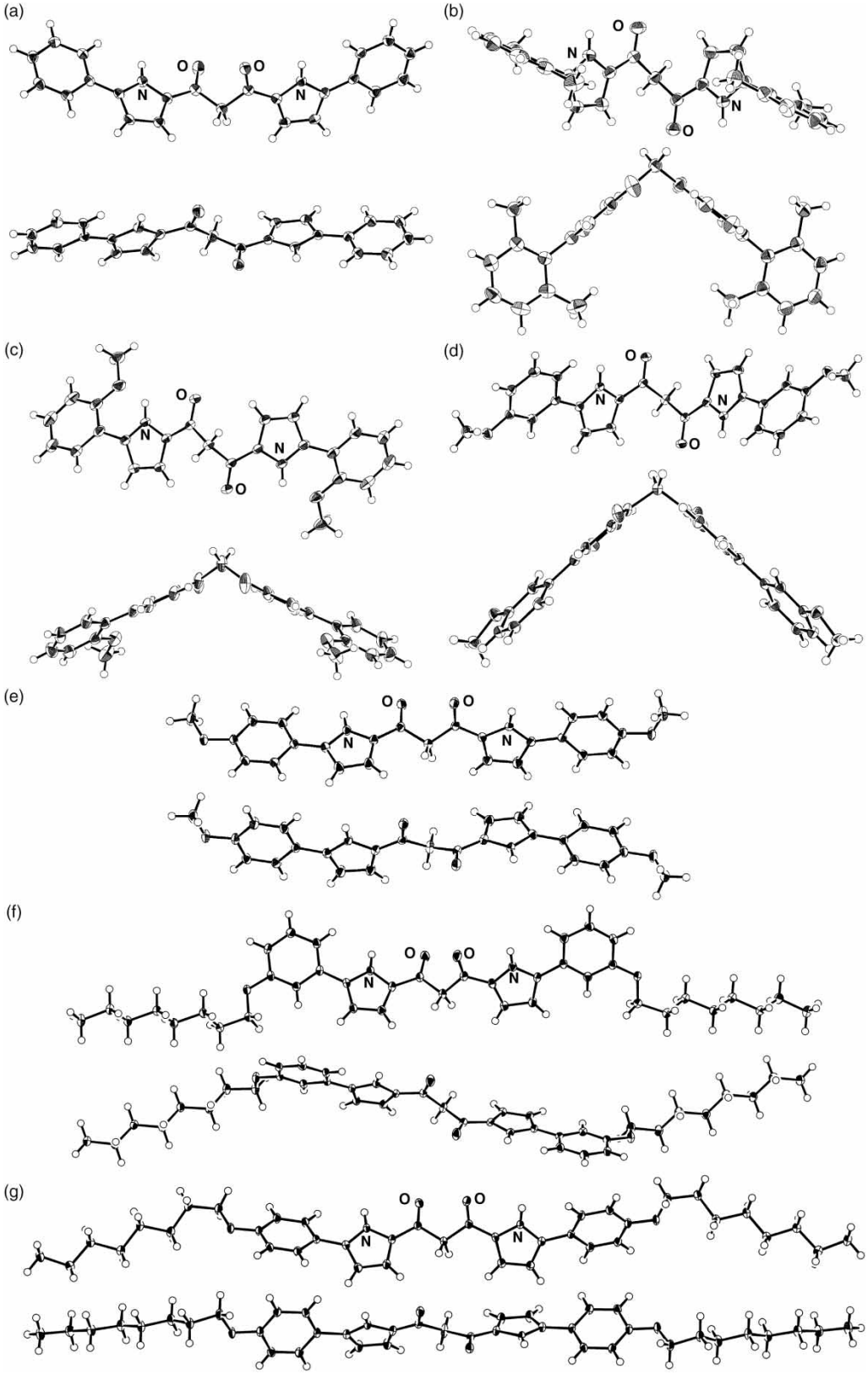

Figure 3. ORTEP drawings (top and side views) of single-crystal X-ray structures of α-aryl-substituted dipyrrolyldiketones: (a) **2a**, (b) **2b**, (c) **3a**, (d) **3b**, (e) **3c**, (f) **3d** and (g) **3e**. Thermal ellipsoids are scaled to the 50% probability level. Solvent molecules are omitted for clarity for **2b**.

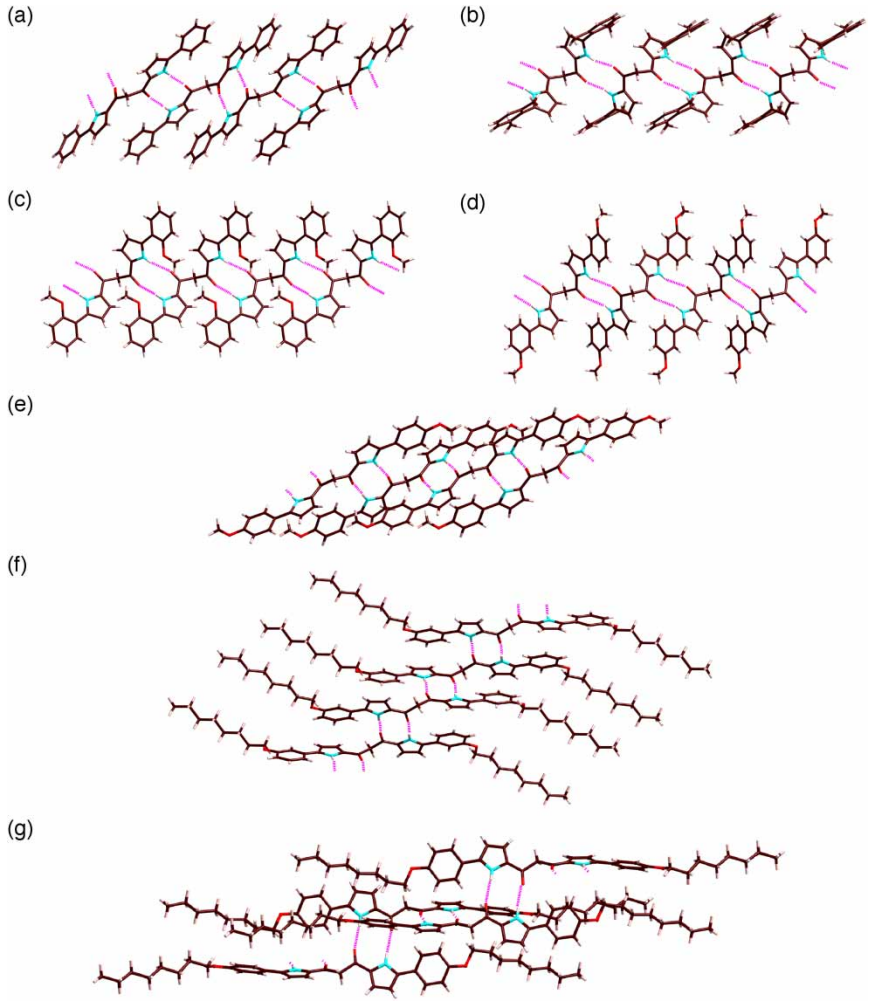

Figure 4. 1D hydrogen-bonding chains of (a) **2a**, (b) **2b**, (c) **3a**, (d) **3b**, (e) **3c**, (f) **3d** and (g) **3e**. Solvent molecules are omitted for clarity for **2b**. Atom colour code: brown, blue, pink and red represent carbon, nitrogen, hydrogen and oxygen, respectively.

2.2 Solid-state keto–enol equilibria of β-alkyl and β-aryl derivatives

Modifications of the molecular structures are crucial for controlling assembled structures and their electronic and optical properties. By focusing on the pyrrole rings, β-substituents can also be effective for the fabrication and control of functionally organised structures (*9r*). We obtained single crystals of β-methyl- and β-ethyl-substituted **4a–c** (*9h,l*), and β-phenyl-substituted **4d** (Figure 5). The diketones **4a**,**b**,**d** were synthesised from the corresponding pyrroles and malonyl chloride in CH_2Cl_2, whereas α-iodo-substituted **4c** was prepared by removal of a boron moiety for the precursory bisiodo-substituted BF_2 complex (*9h*) by treatment with $AlCl_3$ and *tert*-butyl alcohol. In contrast to the single-crystal structures of **1a**, **2a**,**b** and **3a–d**, those of β-alkyl and β-aryl derivatives **4a–d** form enol tautomers in the solid state (Figure 6). The distances between two oxygens of hydrogen-bonding cyclic enol-type 1,3-diketones of **4a–d** are 2.40/2.42, 2.43, 2.48 and 2.42 Å, respectively. The intramolecular dihedral angles between two planes consisting of five atoms (NH and CO with the bridging pyrrole α-C) were estimated to be 6.12°/7.14°, 17.30°, 4.61° and 20.02° for **4a–d**, respectively. Those between two pyrrole rings had almost the same values to each angle of the above planes at 4.99°/5.36°, 27.45°, 2.21° and 33.49° for **4a–d**, respectively. In solutions, the equilibrium between keto and enol forms was observed in **4a–d** as well as in the other derivatives **1a**, **2a**,**b** and **3a–d**; the correlations between the solid and solution states cannot be discussed at present and will be reported elsewhere.

β-Alkyl- and β-aryl-substituted **4a–d** in *cis*-enol forms also provide solid-state assembled structures through hydrogen bonding between pyrrole NH and carbonyl or hydroxy oxygen (Figure 7): the distances between N(H) and carbonyl oxygen in **4a–d** are 2.87, 2.91, 2.95 and 2.83 Å, respectively, whereas those for hydroxy oxygen in **4a**,**b**,**d** are

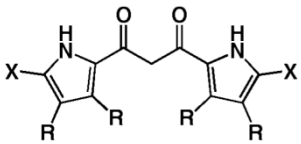

Figure 5. β-Alkyl- and β-aryl-substituted dipyrrolyldiketones **4a**–**d**.

2.92, 2.89 and 2.88 Å, respectively. Among these derivatives, α-iodo-substituted **4c** lacks interaction of pyrrole NH with hydroxy oxygen; instead, it forms N(—H)···I hydrogen bonding with the distance of 3.79 Å. In these cases, as discussed in Section 1, building components are fairly planar due to intramolecular hydrogen bonding. Therefore, hydrogen-bonding chains exhibit tape-like structures, wherein molecules are arranged in a completely parallel and step-like form in **4b** with the distances of 1.34 and 1.97 Å between the neighbouring hydrogen-bonded planar moieties comprising NH, CO and the bridging pyrrole α-C; they are almost parallel in **4d** and are fairly distorted in **4a**,**c**. The dihedral angles between hydrogen-bonding molecules, defined as 15 core atoms of two pyrrole rings and 1,3-propanedione moiety, in **4a**,**c**,**d** are 38.29°/38.31°, 42.31° and 0.97°, respectively. Furthermore, β-methyl-substituted **4a** exhibits infinitely stacking structures of the π-planes at a distance of 3.49 Å, which is defined as the average distance of stacking tetramers each comprising 15 core atoms, while **4c** forms parallel stacking dimers at a distance of 3.45 Å. This is in sharp contrast to **4b**,**d**, which have no significant stacking structures. These observations can be derived from the differences in the substituents, which affect the appropriate packing modes.

3. Experimental section

3.1 General procedures

Starting materials were purchased from Wako Pure Chemical Industries, Ltd. (Osaka, Japan), Nacalai Tesque Inc. (Kyoto, Japan), Sigma-Aldrich Co. (St Louis, MO) and used without further purification unless otherwise stated. NMR spectra used in the characterisation of products were recorded on a JEOL ECA-600 600 MHz spectrometer. All NMR spectra were referenced to solvent. Matrix-assisted laser desorption ionisation time-of-flight mass spectrometries (MALDI-TOF-MS) were recorded on

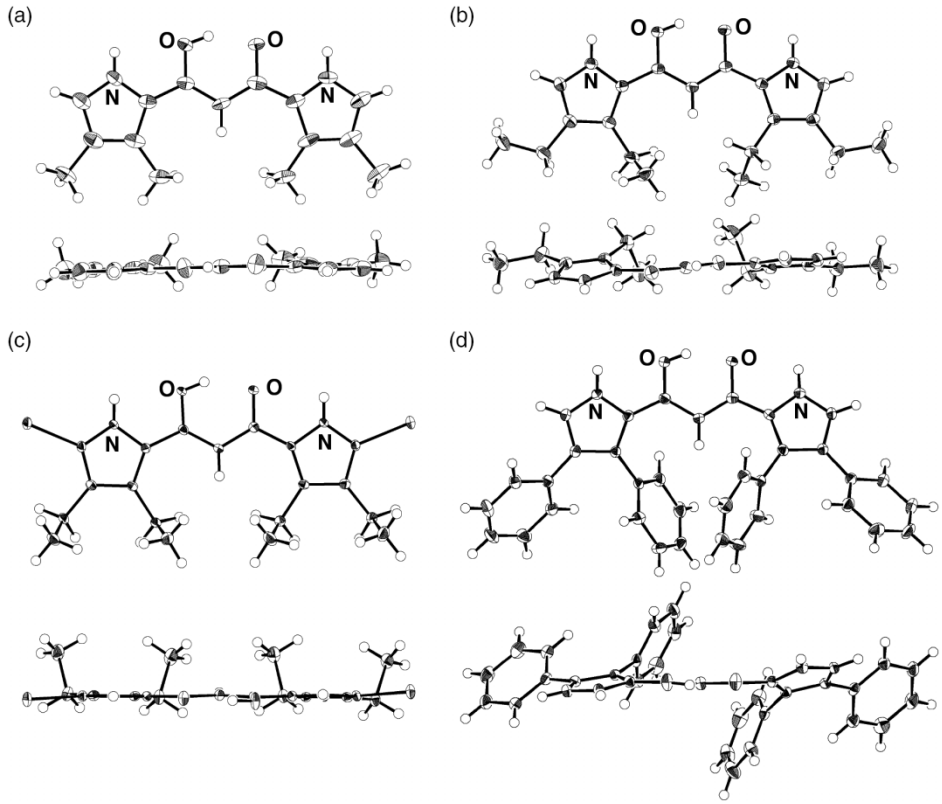

Figure 6. ORTEP drawings (top and side views) of single-crystal X-ray structures of β-alkyl- and β-aryl-substituted dipyrrolyldiketones: (a) **4a** (one of the two independent structures), (b) **4b**, (c) **4c** and (d) **4d**. Thermal ellipsoids are scaled to the 50% probability level. Solvent molecules are omitted for clarity for **4d**. The structure of **4b**, which has been reported as a keto form (*6*), was examined again and solved as a *cis*-enol form.

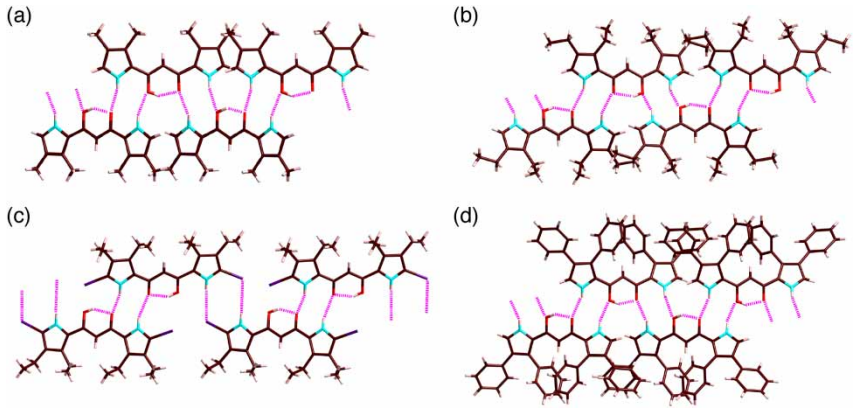

Figure 7. 1D hydrogen-bonding chains of (a) **4a**, (b) **4b**, (c) **4c** and (d) **4d**. Solvent molecules are omitted for clarity for **4d**. Atom colour code: purple represents iodine.

a Shimadzu Axima-CFR plus using negative mode. TLC analyses were carried out on aluminium sheets coated with silica gel 60 (Merck 5554). Column chromatography was performed on Wakogel C-300 and Merck silica gel 60H.

3.2 1,3-Bis-(3,4-diethyl-5-iodopyrrol-2-yl)-1,3-propanedione (4c)

A solution of the BF_2 complex of **4c** (100 mg, 0.16 mmol) in dry CH_2Cl_2 (68 ml) was treated with $AlCl_3$ (129.5 mg, 0.97 mmol) and stirred for 5–10 min at reflux temperature. To the mixture was added *t*-BuOH (4.83 ml, 0.05 mmol) and stirred for 5–10 min at room temperature. To the mixture was added water and stirred for 17 h at the same temperature. The mixture was partitioned between water and CH_2Cl_2, and the combined extracts were dried over anhydrous $MgSO_4$ and evaporated. The residue was then purified by silica gel chromatography (Wakogel C-300, CH_2Cl_2:hexane = 2:1) to give **4c** (34.4 mg, 0.06 mmol, 38%) as a yellow solid. $R_f = 0.32$ (CH_2Cl_2:hexane = 2:1). ^{1}H NMR (600 MHz, $CDCl_3$, 20°C; diketone **4c** was obtained as a mixture of keto and enol tautomers in the ratio of 0.19:1): keto form δ (ppm) 9.88 (s, 2H, NH), 4.17 (s, 2H, CH_2), 2.83 (q, $J = 7.8$ Hz, 4H, CH_2), 2.37 (q, $J = 7.8$ Hz, 4H, CH_2), 1.23 (m, 6H, CH_3), 1.10 (m, 6H, CH_3); enol form δ (ppm) 17.40 (s, 1H, enol-OH), 9.10 (s, 2H, NH), 6.15 (s, 1H, CH), 2.75 (q, $J = 7.8$ Hz, 4H, CH_2), 2.40 (q, $J = 7.8$ Hz, 4H, CH_2), 1.23 (m, 6H, CH_3), 1.10 (m, 6H, CH_3). MALDI-TOF-MS: *m/z* (% intensity): 565.0 (100). Calcd for $C_{19}H_{23}I_2N_2O_2$ ($[M - H]^-$): 564.98.

3.3 1,3-Bis-(3,4-diphenylpyrrol-2-yl)-1,3-propanedione (4d)

Following the literature procedure (*9a*), to a CH_2Cl_2 (7.0 ml) solution of 3,4-diphenylpyrrole (*12*) (108.5 mg, 0.49 mmol) was added malonyl chloride (34.7 mg, 0.25 mmol) at room temperature and stirred for 1.5 h at the same temperature. After the consumption of the starting pyrrole confirmed by TLC analysis, the mixture was washed with saturated aqueous Na_2CO_3 and water, dried over anhydrous Na_2SO_4, filtered and evaporated to dryness. The residue was then chromatographed over a silica gel column (Wakogel C-300, 2% MeOH–CH_2Cl_2) and crystallisation from CH_2Cl_2–hexane afforded **4d** (88.9 mg, 71%) as a pale yellow solid. $R_f = 0.37$ (3% MeOH–CH_2Cl_2). ^{1}H NMR (600 MHz, $CDCl_3$, 20°C; diketone **4d** was obtained as a mixture of keto and enol tautomers in the ratio of 1:0.35): δ (ppm) keto form 9.46 (s, 2H, NH), 7.23–7.11/7.06–6.98 (m, 20H, Ph-H), 7.17 (d, $J = 3.6$ Hz, 2H, pyrrole-H), 3.19 (s, 2H, CH_2); enol form δ (ppm) 16.78 (s, 1H, enol-OH), 9.03 (s, 2H, NH), 7.23–7.11/7.06–6.98 (m, 20H, Ph-H), 7.08 (d, $J = 3.0$ Hz, 2H, pyrrole-H), 5.41 (s, 1H, CH). MALDI-TOF-MS: *m/z* (% intensity): 505.2 (100), 506.2 (79). Calcd for $C_{35}H_{25}N_2O_2$ ($[M - H]^-$): 505.19.

3.4 Single-crystal X-ray analysis

Crystallographic data for dipyrrolyldiketones are summarised in Table 1. All the data were collected at 123 K on a Rigaku RAXIS-RAPID diffractometer with graphite monochromated Mo Kα radiation ($\lambda = 0.71075$ Å); the structure was solved by a direct method. A single crystal of **2a** was obtained by vapour diffusion of hexane into a CH_2Cl_2 solution. The data crystal was a colourless prism of approximate dimensions, 0.40 mm × 0.20 mm × 0.10 mm. A single crystal of **2b** was obtained by vapour diffusion of hexane into a $CHCl_3$ solution with a small amount of toluene. The data crystal was a colourless prism of approximate dimensions, 0.40 mm × 0.30 mm × 0.30 mm. A single crystal of **3a** was obtained by vapour diffusion of hexane into a CH_2Cl_2 solution. The data crystal was a yellow prism of approximate dimensions, 0.45 mm × 0.20 mm × 0.20 mm. A single crystal of **3b** was obtained by vapour diffusion of

Table 1. Crystallographic details for compounds **2a**,**b**, **3a–e** and **4a–d**.

	2a	**2b**	**3a**	**3b**	**3c**	**3d**	**3e**	**4a**	**4b**[a]	**4c**	**4d**
Formula	$C_{23}H_{18}N_2O_2$	$C_{27}H_{26}N_2O_2$ ·0.5$CHCl_3$	$C_{25}H_{22}N_2O_4$	$C_{25}H_{22}N_2O_4$	$C_{25}H_{22}N_2O_4$	$C_{39}H_{50}N_2O_4$	$C_{39}H_{50}N_2O_4$	$C_{15}H_{18}N_2O_2$	$C_{19}H_{26}N_2O_2$	$C_{19}H_{24}I_2N_2O_2$	$C_{35}H_{26}N_2O_2$ ·CH_2Cl_2
fw	354.39	469.68	414.45	414.45	414.45	610.81	610.81	258.31	314.42	566.20	591.50
Crystal size (mm)	0.40 × 0.20 × 0.10	0.40 × 0.30 × 0.30	0.45 × 0.20 × 0.20	0.60 × 0.60 × 0.50	0.50 × 0.20 × 0.20	0.40 × 0.20 × 0.05	0.40 × 0.20 × 0.05	0.60 × 0.40 × 0.30	0.30 × 0.20 × 0.20	0.30 × 0.10 × 0.05	0.40 × 0.20 × 0.20
Crystal system	Triclinic	Orthorhombic	Monoclinic	Monoclinic	Triclinic	Triclinic	Monoclinic	Monoclinic	Monoclinic	Monoclinic	Orthorhombic
Space group	$P\bar{1}$ (no. 2)	*Pbcn* (no. 60)	*C*2/*c* (no. 15)	*C*2/*c* (no. 15)	$P\bar{1}$ (no. 2)	$P\bar{1}$ (no. 2)	*C*2/*c* (no. 15)	$P2_1/n$ (no. 14)	$P2_1/n$ (no. 14)	*P*2/*n* (no. 13)	*F*2*dd* (no. 43)
a (Å)	5.530 (3)	14.095 (4)	16.144 (14)	28.995 (19)	9.070 (5)	6.928 (2)	32.881 (10)	14.619 (9)	11.444 (4)	14.386 (5)	10.942 (3)
b (Å)	11.714 (6)	14.951 (4)	18.27 (3)	4.952 (2)	10.782 (6)	10.995 (5)	8.636 (3)	10.370 (8)	10.861 (4)	9.082 (3)	32.709 (7)
c (Å)	13.661 (9)	23.246 (6)	7.183 (9)	14.049 (7)	11.625 (5)	22.002 (8)	11.899 (5)	18.937 (13)	14.563 (8)	15.330 (6)	33.875 (8)
α (°)	81.86 (2)	90	90	90	75.049 (19)	86.724 (16)	90	90	90	90	90
β (°)	82.10 (3)	90	110.67 (2)	101.00 (3)	69.072 (19)	85.505 (12)	99.553 (15)	112.50 (2)	107.135 (16)	102.775 (15)	90
γ (°)	85.66 (2)	90	90	90	86.50 (2)	87.823 (16)	90	90	90	90	90
V (Å^3)	866.3 (9)	4899 (2)	1983 (4)	1980.0 (18)	1025.3 (9)	1667.3 (11)	3332 (2)	2652 (3)	1729.6 (13)	1953.4 (12)	12124 (5)
ρ_{calcd} (g cm^{-3})	1.359	1.274	1.389	1.390	1.343	1.217	1.218	1.294	1.207	1.925	1.296
Z	2	8	4	4	2	2	4	8	4	4	16
T (K)	123 (2)	123 (2)	123 (2)	123 (2)	123 (2)	123 (2)	123 (2)	123 (2)	123 (2)	123 (2)	123 (2)
μ(Mo-Kα), (mm^{-1})	0.088	0.237	0.095	0.095	0.092	0.078	0.078	0.087	0.078	3.235	0.250
No. of reflections	8525	42,635	9681	8987	10,153	16,520	15,791	15,231	15,942	18,350	27,460
No. of unique reflections	3908	5622	2278	2260	4654	7552	3802	4672	3909	4461	6796
Variables	245	307	142	142	282	408	205	351	213	232	390
$\lambda_{Mo\text{-}K\alpha}$ (Å)	0.71075	0.71075	0.71075	0.71075	0.71075	0.71075	0.71075	0.71075	0.71075	0.71075	0.71075
R_1 ($I > 2\sigma(I)$)	0.0484	0.0798	0.0441	0.0392	0.0409	0.0441	0.0487	0.0982	0.0444	0.0192	0.0402
wR_2 ($I > 2\sigma(I)$)	0.1059	0.2254	0.1142	0.1064	0.1064	0.1276	0.1129	0.2493	0.1100	0.0423	0.0891
GOF	1.041	1.057	1.081	1.095	1.071	1.041	1.030	1.144	1.052	1.080	1.033

[a]Revised data of that reported in ref. (*11*).

hexane into a CH_2Cl_2 solution. The data crystal was a yellow prism of approximate dimensions, 0.60 mm × 0.60 mm × 0.50 mm. A single crystal of **3c** was obtained by vapour diffusion of hexane into a CH_2Cl_2 solution. The data crystal was a red block of approximate dimensions, 0.50 mm × 0.20 mm × 0.20 mm. A single crystal of **3d** was obtained by vapour diffusion of MeOH into a $CDCl_3$ solution. The data crystal was a yellow prism of approximate dimensions, 0.80 mm × 0.30 mm × 0.10 mm. A single crystal of **3e** was obtained by vapour diffusion of MeOH into a $CHCl_3$ solution. The data crystal was a yellow prism of approximate dimensions, 0.40 mm × 0.20 mm × 0.05 mm. A single crystal of **4a** was obtained by vapour diffusion of hexane into a CH_2Cl_2 solution. The data crystal was a yellow prism of approximate dimensions, 0.60 mm × 0.40 mm × 0.30 mm. A single crystal of **4b** was obtained by vapour diffusion of hexane into a CH_2Cl_2 solution. The data crystal was a yellow prism of approximate dimensions, 0.30 mm × 0.20 mm × 0.20 mm. A single crystal of **4c** was obtained by vapour diffusion of hexane into a CH_2Cl_2 solution. The data crystal was a yellow prism of approximate dimensions, 0.30 mm × 0.10 mm × 0.05 mm. A single crystal of **4d** was obtained by vapour diffusion of hexane into a CH_2Cl_2 solution with a small amount of toluene. The data crystal was a yellow prism of approximate dimensions, 0.40 mm × 0.20 mm × 0.20 mm. In each case, the non-hydrogen atoms were refined anisotropically. The calculations were performed using the Crystal Structure crystallographic software package of Molecular Structure Corporation. CIF files (CCDC-626137 for **4b** (a revised structure), 664473 and 664474 for **2a** and **2b**, respectively and 782949–782956 for **3a**–**e** and **4a**,**c**,**d**) can be obtained free of charge from the Cambridge Crystallographic Data Centre via www.ccdc.cam.ac.uk/data_request/cif

4. Summary

As observed in a parent structure, α-aryl-substituted 1,3-dipyrrolyl-1,3-propanedione (dipyrrolyldiketone) derivatives prefer keto tautomers and form solid-state 1D hydrogen-bonding chain structures, whose geometries differ according to the substituents. In contrast, β-alkyl- and β-aryl-substituted derivatives stabilise the *cis*-enol forms in the solid state, resulting in the formation of 1D hydrogen-bonding chains. At present, although it is not easy to discuss the details of the correlation of pyrrole substituents with tautomeric forms in the solid state, the existence of β-substituents seems to influence the packing structures and, as a result, preferred tautomeric forms. A series of dipyrrolyldiketones, the building subunits for molecular assemblies, afford complexes with not only boron but also various metal cations that exhibit fascinating electronic and optical properties along with the formation of functional materials. Further investigation to prepare various metal complexes is under way.

Acknowledgements

This work was supported by Ritsumeikan Global Innovation Research Organization (R-GIRO) Project (2008-2013). The authors thank Prof. Atsuhiro Osuka, Dr Shigeki Mori, Dr Shohei Saito, Mr Eiji Tsurumaki, Mr Taro Koide and Mr Takayuki Tanaka, Kyoto University, for single-crystal X-ray analyses and Prof. Hitoshi Tamiaki, Ritsumeikan University, for various measurements. Y.H. thanks JSPS for a Research Fellowship for Young Scientists.

References

(1) Jeffrey, G.A.; Saenger, W. *Hydrogen Bonding in Biological Structures*; Springer: Berlin, Germany, 1991.
(2) Prins, L.J.; Timmerman, P.; Reinhoudt, D.N. *Angew. Chem., Int. Ed.* **2001**, *40*, 2382–2426.
(3) Reichardt, C. *Solvents and Solvent Effects in Organic Chemistry*; Wiley: Weinheim, 2003; Chapter 4.
(4) (a) Kadish, K.M., Smith, K.M., Guilard, R., Eds.; *The Porphyrin Handbook*; Academic Press: San Diego, CA, 2000; (b) Kadish, K.M., Smith, K.M., Guilard, R., Eds.; *Handbook of Porphyrin Science*; World Scientific: Hackensack, NJ, 2010.
(5) (a) Sessler, J.L.; Camiolo, S.; Gale, P.A. *Coord. Chem. Rev.* **2003**, *240*, 17–55; (b) Gale, P.A. *Chem. Commun.* **2005**, 3761–3772.
(6) (a) Sessler, J.L.; Weghorn, S.J.; Hiseada, Y.; Lynch, V. *Chem. Eur. J.* **1995**, *1*, 56–67; (b) Scherer, M.; Sessler, J.L.; Gebauer, A.; Lynch, V. *J. Org. Chem.* **1997**, *62*, 7877–7881; (c) Scherer, M.; Sessler, J.L.; Moini, M.; Gebauer, A.; Lynch, V.M. *Chem. Eur. J.* **1998**, *4*, 152–158; (d) Sessler, J.L.; Berthon-Gelloz, G.; Gale, P.A.; Camiolo, S.; Anslyn, E.V.; Anzenbacher, P. Jr.; Furuta, H.; Kirkovits, G.J.; Lynch, V.M.; Maeda, H.; Morosini, P.; Scherer, M.; Shriver, J.; Zimmerman, R.S. *Polyhedron* **2003**, *22*, 2963–2983; (e) Schmuck, C.; Wienand, W. *J. Am. Chem. Soc.* **2003**, *125*, 452–459; (f) Uno, H.; Ito, S.; Wada, M.; Watanabe, H.; Nagai, M.; Hayashi, A.; Murashima, T.; Ono, N. *J. Chem. Soc., Perkin Trans. 1* **2000**, 4347–4355.
(7) (a) Oddo, B.; Dainotti, C. *Gazz. Chim. Ital.* **1912**, *42*, 716–726; (b) Stark, W.M.; Baker, M.G.; Leeper, F.J.; Raithby, P.R.; Battersby, A.R. *J. Chem. Soc., Perkin Trans. 1* **1988**, 1187–1201.
(8) (a) Maeda, H. *Eur. J. Org. Chem.* **2007**, 5313–5325; (b) Maeda, H. *Chem. Eur. J.* **2008**, *14*, 11274–11282; (c) Maeda, H. *J. Incl. Phenom.* **2009**, *64*, 193–214; (d) Maeda, H. In *Handbook of Porphyrin Science*; Kadish, K.M., Smith, K.M., Guilard, R., Eds.; World Scientific: Hackensack, NJ, 2010; Vol. 8, Chapter 38; (e) Maeda, H. In *Anion Complexation by Supramolecular Chemistry. Topics in Heterocyclic Chemistry*; Gale, P.A., Dehaen, W., Eds.; Springer-Verlag: Berlin, Germany, 2010; Vol. 24, pp 103–144; (f) Maeda, H. In *Supramolecular Soft Matter: Applications in Materials and Organic Electronics*; Nakanishi, T., Ed.; Wiley, submitted.
(9) (a) Maeda, H.; Kusunose, Y. *Chem. Eur. J.* **2005**, *11*, 5661–5666; (b) Fujimoto, C.; Kusunose, Y.; Maeda, H. *J. Org. Chem.* **2006**, *71*, 2389–2394; (c) Maeda, H.; Ito, Y. *Inorg. Chem.* **2006**, *45*, 8205–8210; (d) Maeda, H.; Kusunose, Y.; Mihashi, Y.; Mizoguchi, T. *J. Org. Chem.* **2007**, *72*, 2612–2616; (e) Maeda, H.; Haketa, Y.; Nakanishi, T. *J. Am. Chem. Soc.* **2007**, *129*, 13661–13674; (f) Maeda, H.; Kusunose, Y.; Mihashi, Y.; Mizoguchi, T. *J. Org. Chem.* **2007**, 72, 2612–2616; (g) Maeda, H.; Terasaki, M.; Haketa, Y.;

Mihashi, Y.; Kusunose, Y. *Org. Biomol. Chem.* **2008**, *6*, 433–436; (h) Maeda, H.; Fujii, Y.; Mihashi, Y. *Chem. Commun.* **2008**, 4285–4287; (i) Maeda, H.; Haketa, Y. *Org. Biomol. Chem.* **2008**, *6*, 3091–3095; (j) Maeda, H.; Mihashi, Y.; Haketa, Y. *Org. Lett.* **2008**, *10*, 3179–3182; (k) Maeda, H.; Ito, Y.; Haketa, Y.; Eifuku, N.; Lee, E.; Lee, M.; Hashishin, T.; Kaneko, K. *Chem. Eur. J.* **2009**, *15*, 3706–3719; (l) Maeda, H.; Haketa, Y.; Bando, Y.; Sakamoto, S. *Synth. Met.* **2009**, *159*, 792–796; (m) Maeda, H.; Eifuku, N. *Chem. Lett.* **2009**, *38*, 208–209; (n) Maeda, H.; Fujii, R.; Haketa, Y. *Eur. J. Org. Chem.* **2010**, 1469–1482; (o) Maeda, H.; Terashima, Y.; Haketa, Y.; Asano, A.; Honsho, Y.; Seki, S.; Shimizu, M.; Mukai, H.; Ohta, K. *Chem. Commun.* **2010**, *46*, 4559–4561; (p) Maeda, H.; Takayama, M.; Kobayashi, K.; Shinmori, H. *Org. Biomol. Chem.* **2010**, *8*, 4308–4315; (q) Maeda, H.; Bando, Y.; Haketa, Y.; Honsho, Y.; Seki, S.; Nakajima, H.; Tohnai, N. *Chem. Eur. J.* **2010**, *16*, in press; Doi: 10.1002/chem201001852; (r) Haketa, Y.; Sakamoto, S.; Nakanishi, T.; Maeda, H. submitted; (s) Haketa, Y.; Maeda, H. submitted.

(10) Maeda, H.; Ito, Y.; Kusunose, Y.; Nakanishi, T. *Chem. Commun.* **2007**, 1136–1138.

(11) Maeda, H.; Kusunose, Y.; Terasaki, M.; Ito, Y.; Fujimoto, C.; Fujii, R.; Nakanishi, T. *Chem. Asian J.* **2007**, *2*, 350–357.

(12) (a) Sera, A.; Fukumoto, S.; Tamura, M.; Takabatake, K.; Yamada, H.; Ito, K. *Bull. Chem. Soc. Jpn.* **1991**, *64*, 1787–1791; (b) Ono, N.; Miyagawa, H.; Ueta, T.; Ogawa, T.; Tani H. *J. Chem. Soc., Perkin Trans. 1* **1998**, 1595–1601.